



OTC-31712-MS

Early Detection and Assessment of Asphaltene Precipitation and Gas Hydrate Formation at Field Conditions

Jose G. Delgado-Linares, Mathias Pohl, and Ahmad A. A. Majid, Colorado School of Mines; Chitose Yoda and Norio Tanaka, Yokogawa Electric Corporation, Omega Simulation Co., Ltd; Luis E. Zerpa, Manika Prasad, and Carolyn A. Koh, Colorado School of Mines

Copyright 2022, Offshore Technology Conference DOI [10.4043/31712-MS](https://doi.org/10.4043/31712-MS)

This paper was prepared for presentation at the Offshore Technology Conference held in Houston, TX, USA, 2 – 5 May, 2022.

This paper was selected for presentation by an OTC program committee following review of information contained in an abstract submitted by the author(s). Contents of the paper have not been reviewed by the Offshore Technology Conference and are subject to correction by the author(s). The material does not necessarily reflect any position of the Offshore Technology Conference, its officers, or members. Electronic reproduction, distribution, or storage of any part of this paper without the written consent of the Offshore Technology Conference is prohibited. Permission to reproduce in print is restricted to an abstract of not more than 300 words; illustrations may not be copied. The abstract must contain conspicuous acknowledgment of OTC copyright.

Abstract

The detection of asphaltene precipitation and gas hydrate formation is critical to preventing production losses and to optimize strategies for mitigation and remediation. Likewise, the evaluation of some flow properties (e.g., viscosity and yield stress) of the slurries formed for asphaltenes and hydrates are paramount when developing and testing prediction tools for safe field operations. Several complications must be considered when dealing with asphaltenes and hydrates at field conditions, e.g., harsher conditions (especially high or extremely high pressure), the variation of fluid composition over time, and the lack of information on the thermodynamic conditions at which those solids (asphaltenes and hydrates) form. One possibility to face this challenge is to use field information to calibrate existing prediction models/tools and make them applicable for new field conditions. Hence, there is interest in industry to develop new tools that allow the detection of asphaltenes and hydrates in the early stages of their formation.

In this work, acoustic and nuclear magnetic resonance (NMR) measurements are utilized to detect asphaltene precipitation in crude and model oils. Asphaltene detection was performed at ambient pressure and at CO₂ pressurized conditions. Acoustic and NMR measurements were sensitive to the asphaltene concentration in the tested oils. In addition, rheological properties such as viscosity and yield stress were determined for hydrate slurries in crude oil systems at different water volume fractions, salt (NaCl) concentrations and gas compositions. Gas hydrate slurry formed from a CO₂-rich gas exhibited a phase inversion in rheological experiments (external phase changed from oil to water), which was possibly promoted by the CO₂-activated natural surfactants of the crude oil.

Introduction

Solids such as asphaltenes and hydrates represent a serious problem in the crude oil production process. Those solids may reduce or even arrest hydrocarbon production due to blockage of transmission lines (Ellison *et al.*, 2000; Gudmundsson, 2017). Given that asphaltenes and hydrates form by different mechanisms with significantly different time scales, the effectiveness of the avoidance/mitigation strategies

strongly depends on the knowledge of the thermodynamic and kinetic conditions of their formation and the accuracy of the detection techniques applied in the field.

Asphaltenes represent the heaviest and most polar crude oil fraction. From an operational point of view, they are defined as the group of compounds insoluble in small paraffins (e.g., pentane or heptane) and soluble in aromatic solvents (e.g., toluene or xylene) (Speight, 2004). Asphaltene molecular structure has been subject of debate for many years; however, currently a general consensus seems to be that the main asphaltene molecule is composed of a polyaromatic core (with ~6 benzene rings) linked to several aliphatic branches with a average molecular weight of ~750 Da. Heteroatoms, such as oxygen, nitrogen, sulphur and metals are responsible for the asphaltene polarity and for the aggregation tendency of this crude oil fraction (Mullins, 2011; Spiecker et al., 2003). Besides their precipitation and deposition in the petroleum reservoir or in the production tubing, asphaltenes also play a major role in the stabililization of water-in-crude oil emulsions (Aguilera et al., 2010; Alimohammadi et al., 2019; Czarnecki & Moran, 2005; Kokal, 2005; McLean & Kilpatrick, 1997).

The asphaltene precipitation occurs when the solubilization power of the medium is reduced and asphaltene molecules self-associate, forming aggregation structures of high molecular weight and eventually a new solid phase (Buckley et al., 2007; Hammami & Ratulowski, 2007). The sequence of steps involved in asphaltene aggregation has been established in the Yen-Mullins model, which presents four main aggregation stages, as shown in Figure 1 (Chen et al., 2020):

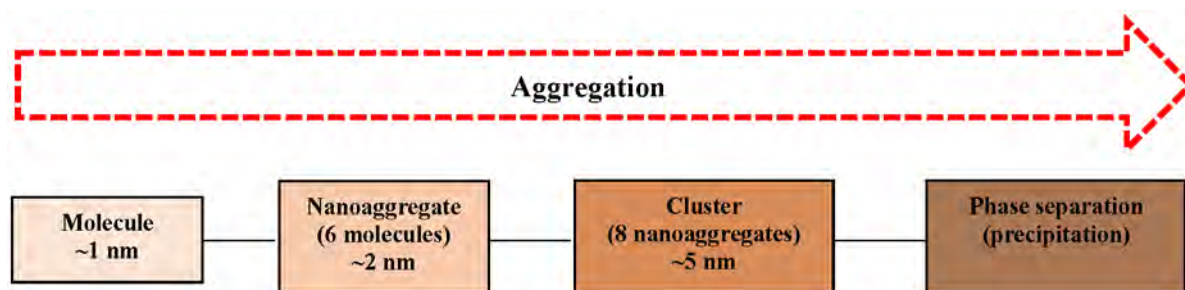


Figure 1—Schematic of Yen-Mullins model of asphaltenes, indicating the different stages of asphaltene aggregation.

The reduction in asphaltene solubility may be induced mainly by: a) addition of liquid paraffinic hydrocarbons, b) pressure reduction close to the crude oil bubble point, and c) addition of CO₂. In all the three situations, a local composition change is induced and the solvent capacity of the oil towards asphaltenes decreases, and thus the aggregation/precipitation mechanisms can take place (da Silva et al., 2014; Hammami & Ratulowski, 2007; Wang et al., 2017). Likewise, it has been demonstrated that in general the precipitation of asphaltenes increases with the CO₂ concentration in the system (Deo & Parra, 2012; Fakher et al., 2020; Lei et al., 2010; Zanganeh et al., 2012).

Asphaltene detection at field conditions is a challenge faced by the industry due mainly to the high-pressures encountered in problematic locations. With the aim to overcome this problem, several techniques have been developed, namely: a) gravimetric measurements, b) acoustic resonance, c) light scattering, and d) filtration. All of these techniques show some potential application, however aspects such as the lack of sensitivity, subjective interpretation, or being time consuming are the main drawbacks in considering them as a definitive solution (Jamaluddin et al., 2002). It is worth mentioning that the accurate detection of the asphaltene precipitation and deposition in the early stages allows for the effective application for remediation/avoidance techniques, e.g., injection of aromatic solvents or chemical dispersants (Gharbi et al., 2017; Kelland, 2016).

Gas hydrates are inclusion solid compounds in which small molecules (e.g., methane or CO₂) are trapped by a hydrogen-bonded network. In general, they occur at low temperatures and high pressures (Sloan & Koh, 2007), which are very common conditions encountered in oil and gas production lines, mainly in

offshore facilities. The operation within the hydrate equilibrium region, even for a short period of time, represents a risk given that the formation of hydrate plugs is relatively fast (Ellison et al., 2000). During hydrate formation/plugging in systems where oil is the dominant phase (e.g., crude oil systems), four main processes take place: a) water emulsification into the oil phase, b) rapid formation of small hydrate "balloons" composed of partially converted water droplets, c) interaction of hydrate particles through capillary bridging, and d) extensive hydrate agglomeration. The occurrence of those processes may be detected by the change of some fluid properties, such as liquid viscosity (Sloan, 2010; Sum et al., 2012).

Hydrate mitigation strategies may be classified in one of the two following categories: avoidance or management. Hydrate avoidance aims to keep the system outside of the region of hydrate equilibrium. This goal can be accomplished by injecting thermodynamic hydrate inhibitors (THIs) such as methanol or mono ethylene glycol (MEG). Inorganic salts (e.g., NaCl) act as THIs shifting the hydrate formation conditions towards lower temperatures and higher pressures. On the other hand, hydrate management allows operation within the hydrate stability region by increasing the time necessary for hydrate formation or reducing the tendency of hydrate particles to agglomerate (Kinnari et al., 2014; Sloan & Koh, 2007). This requires the use of kinetic hydrate inhibitors (KHI) and/or anti-agglomerants (AAs), respectively. In some crude oils, natural antiagglomeration can be used as an alternative of hydrate control with no or minimum addition of commercial chemicals (Delgado-Linares et al., 2021; Salmin et al., 2021).

As shown above, the ability for early detection of asphaltene precipitation/deposition and hydrate formation is critical to prevent losses in crude oil production. These flow assurance solids can occur simultaneously or in different stages of the production process. The application of mitigation methods just when asphaltenes and hydrates start to appear could reduce the OPEX due to remediation treatments. Moreover, the evaluation of flow behavior of the slurries generated by those flow assurance solids is also key in quantifying the energy required for their transportation. In this work, acoustic velocity and nuclear magnetic resonance (NMR) measurements were used to infer asphaltene precipitation and aggregation in crude oils and model systems. The use of these techniques in laboratory experiments constitutes the initial step for their further application in the field. Likewise, hydrate formation / flow measurements were performed to quantitatively assess the slurry rheological properties of hydrate systems under both steady state and transient (shut-in/re-start) conditions.

Methods and Materials

Oils

Crude oils. Two crude oils labeled as N1-C and N1-A were used in this study. Table 1 shows some physical properties of these oils. Since crude N1-A is an unstable crude oil with asphaltenes originally precipitated, it was used in experiments where solid asphaltenes in crude oil are needed.

Table 1—Physical properties of the crude oils used

Crude oil	API gravity	Asphaltene content (wt.%)
N1-C	20	2.5
N1-A	29	4.5

Model oil. In experiments carried out with model systems, asphaltenes were dissolved in a mixture toluene-heptane (heptol). Asphaltenes were separated from the crude oil N1-C by adding n-heptane in a heptane/crude oil ratio (mL/g) of 40. This separation process has been published elsewhere (Aguilera et al., 2010; Reyes Molina et al., 2021) and is based on the standard IP 143.

Asphaltenes were dissolved in toluene through ultrasonic stirring bath (60 Hz) for 12 minutes. The complete dissolution was verified by using an optical microscope. Heptane was then added, and the sample was stirred in an ultrasonic bath for 4 additional minutes. This kind of model oil has been previously used to study asphaltene precipitation (Zanganeh et al., 2012).

De-asphalted oil. A sample of crude N1-A was mixed with heptane in a ratio 20/1 (mL of heptane / grams of crude oil) and mixed with a magnetic stirrer for 10 mins. The mixture was filtered with a 2.5 μm filter paper to separate the precipitated solid from the maltenes (de-asphalted oil). Heptane was separated from the de-asphalted oil in a rotary evaporator under vacuum condition. The absence of solids was confirmed by using an optical microscope. Acoustic measurements with de-asphalted crude oil N1-A were compared with the whole crude oil in which solid asphaltenes are originally present.

Gases

Three kinds of gases were used in this work, namely CO_2 , natural gas, and CO_2 -rich gas. Table 2 depicts the composition of the gas mixtures.

Table 2—Composition of the gas mixtures used in this study

Composition	Mole percent (%)	
	Natural gas	CO_2 -rich gas
Carbon dioxide (CO_2)	7.14	43.80
Methane	79.69	49.80
Ethane	7.14	3.00
Propane	4.00	2.00
Butane	2.03	1.40

Acoustic measurements

Acoustic measurements were carried out at ambient and at high pressure (500 psig) on model oils (with asphaltenes from crude N1-C) and crude oil N1-A (with and without asphaltenes). By knowing the length of the sample and the time it takes for the wave to travel such a length, the velocity in the oil was calculated. In these experiments, sample holders were used with one transducer on the top and one on the bottom. One of the transducers serves as a source, which generates an acoustic wave, and the second transducer serves as a receiver which records the wave.

To generate the acoustic signal, a pulser is used, and the acoustic wave is digitized on an oscilloscope. Changes in arrival time as well as wave amplitudes due to the presence of precipitated/deposited asphaltenes were investigated. Benchtop measurements were conducted on crude N1-A (with and without asphaltenes) and pressurized experiments (500 psi of CO_2) were performed on the model oil (toluene 70% - heptane 30%) with varying asphaltene content (asphaltenes from crude N1-C). It is worth noting that asphaltenes are in a dissolved state at ambient conditions and precipitation could be induced by pressurizing the system with CO_2 gas.

Nuclear magnetic resonance (NMR)

Ambient and pressurized low field NMR experiments (2 MHz) (Livo et al., 2021) were carried out on oil samples that contained asphaltenes (crude oil N1-A, and model oil with 0, 1, 2.5, and 4 wt.% asphaltenes from crude N1-C), as well as on a sample of de-asphalted oil N1-A. T2 relaxation curves were recorded to observe the changes in relaxation time with and without asphaltenes. Model oils with dissolved asphaltenes were pressurized with CO_2 to induce asphaltene precipitation. The effect of different asphaltene contents in

the model oil on T2 relaxations was analyzed. More details regarding the experimental setup can be found in [Livo et al. \(2021\)](#).

Emulsion preparation for hydrate tests

Emulsions were prepared by homogenizing the water into the oil phase at 8,000 rpm for 3 mins. The water was added dropwise using a syringe during the first minute. This protocol has been used in several published works ([Delgado-Linares et al., 2013](#), [Delgado-Linares et al., 2020](#); [Sjöblom et al., 2010](#)).

Emulsion stability in presence of hydrates. High-Pressure Differential Scanning Calorimetry (HP-DSC)

Emulsion stability under gas hydrate formation and dissociation was studied by using a microdifferential scanning calorimeter. In this work, a low emulsion stability under the hydrate formation and dissociation pathways is an indication of high hydrate particle agglomeration ([Majid et al., 2021](#)). In this method, ~15 mg of emulsion sample was needed for evaluation of emulsion stability. The HP-DSC setup has an operating temperature of -45 to 120 °C and maximum operating pressure of 2,200 psi (15.2 MPa). In these tests, the sample was cooled from 30 °C to the experimental temperature (-5 °C) to form hydrates. The sample was then heated back to 30 °C to dissociate the hydrates. These cooling and heating steps (hydrate formation and dissociation) were repeated for an additional two times. The stability of the emulsion upon hydrate formation and dissociation was evaluated by comparing the amount of hydrates formed in each formation/dissociation cycle.

Rheological measurements of gas hydrate slurries

Rheological properties of hydrate slurries, such as viscosity and yield stress, were measured using a high-pressure rheometer. The apparatus has an operating shear rate of 0.1 to 1000 s⁻¹, an operating temperature of -40 to 150 °C and can withstand pressures of up to 2000 psi (14 MPa). The high-pressure rheometer is connected to a high-pressure syringe pump to control the pressure of the system and monitor the gas consumption (for hydrate formation and gas solubilization). In this work, 30 ml of emulsion sample was injected into the high-pressure rheometer cell. The system was then pressurized up to 1000 psig. The sample was stirred at the constant shear outside the hydrate equilibrium condition (20 °C) for 90 minutes to saturate the oil phase. Two gas compositions were used in this investigation: (1) natural gas composition and (2) CO₂-rich natural gas composition ([Table 2](#)).

After full saturation, the sample was cooled to the experimental temperature (4 °C) at a rate of 0.5 °C/min for hydrate formation. The sample was stirred at this condition for 55 hours. Following this step, the sample was put into a shut-in condition (no stirring) for 24 hours. Next, a shear force was slowly exerted upon the sample to determine the yield stress of the slurries ([Majid et al., 2017](#); [Rensing et al., 2011](#)). After the yield stress measurements, ramping tests were conducted whereby the stirring speed was increased and decreased to observe any hysteresis.

Results and discussion

Asphaltene detection through acoustic measurements

The recorded benchtop acoustic waveforms for crude oil N1-A can be seen in [Figure 2](#). Changes in velocity (inferred from the wave arrival time) were observed in the presence and absence of asphaltenes. The calculated velocities were lower by 70 m/s (~5%) when asphaltenes were present. The presence of solid asphaltene particles delayed the acoustic wave arrival, decreasing its velocity. Additionally, a reduction in amplitude after 2 μs was observed in the oil sample that contains asphaltenes suggesting potential effects of the precipitated asphaltenes on the later part of the acoustic wave, also called the coda.

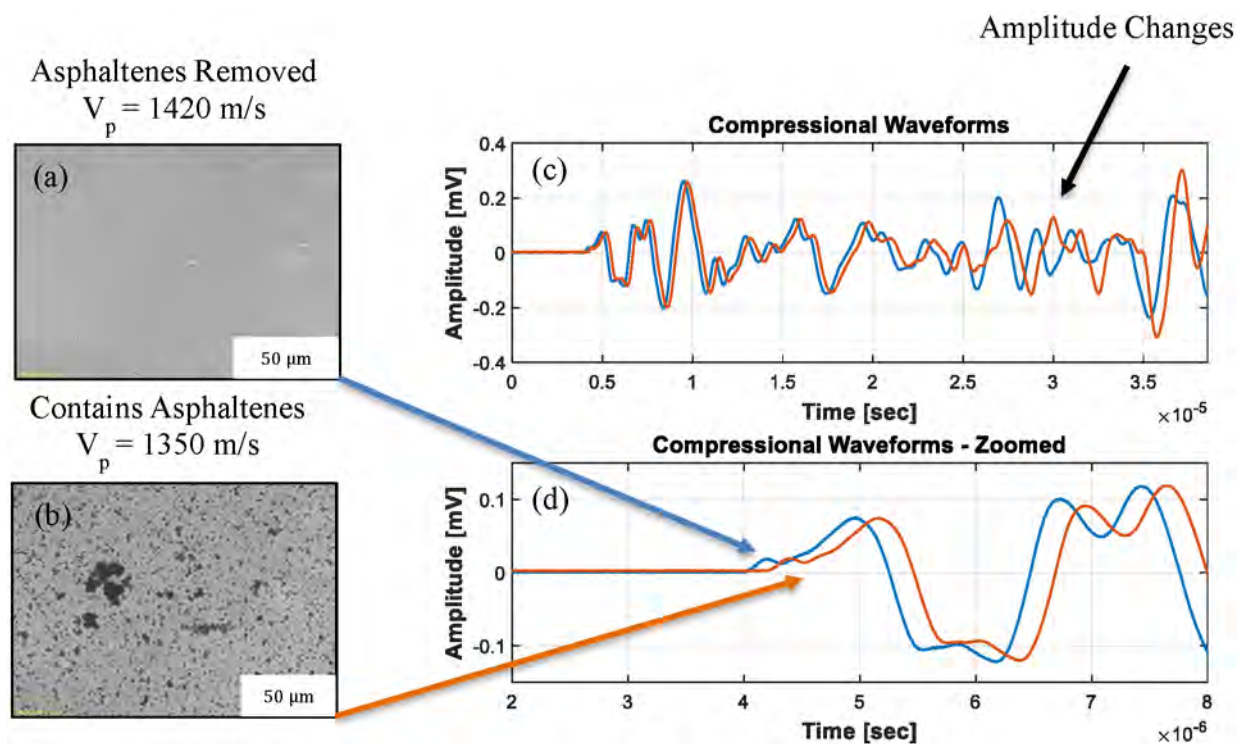


Figure 2—(a) De-asphalted N1-A oil (b) As-is N1-A oil (c) entire wave track for the as-is N1-A crude oil (red) and de-asphalted N1-A oil (blue) (d) zoomed wave track for the as-is N1-A crude oil (red) and de-asphalted N1-A oil (blue)

These changes indicate a loss in energy and wave velocity as the acoustic wave reverberates in the sample and small effects in the acoustic path accumulate as the wave covers multiple paths in the sample. The cumulative effect is enhanced at increasing times (Figure 2).

Figure 3 shows results for the system pressurized with CO_2 gas (500 psig) with model oil (toluene 70% - heptane 30%) with varying asphaltene contents from crude N1-C. Time equals zero indicates measurements at ambient conditions before pressurization with CO_2 . The velocities decrease with increasing asphaltene content as the density of the model oil mixture increases. Injection of CO_2 decreased the velocities for all three samples immediately. The largest decrease was observed for the model oil containing the highest amount of asphaltenes (Table 3). Moreover, changes in the acoustic waveforms and arrival times (Figure 4) can be observed continuously for samples containing asphaltenes from crude N1-C (2.5 wt.% - Figure 4b), whereas the sample containing no asphaltenes (0 wt.% - Figure 4a) showed only minor changes. The largest drop in velocities occur immediately after CO_2 gas is introduced to the system. CO_2 molecules dissolve into the model oil and cause asphaltenes to precipitate.

Table 3—Percentage changes in velocity for model oils with different asphaltene content

	Asphaltene content			
	0 wt.%	2.5 wt.%		4 wt.%
% Change after 1 h (compared to initial velocity)		4.4	4.4	14.4
% Change after 24h (compared to initial velocity)		4.3*	6.6	18.5

*after 22 h

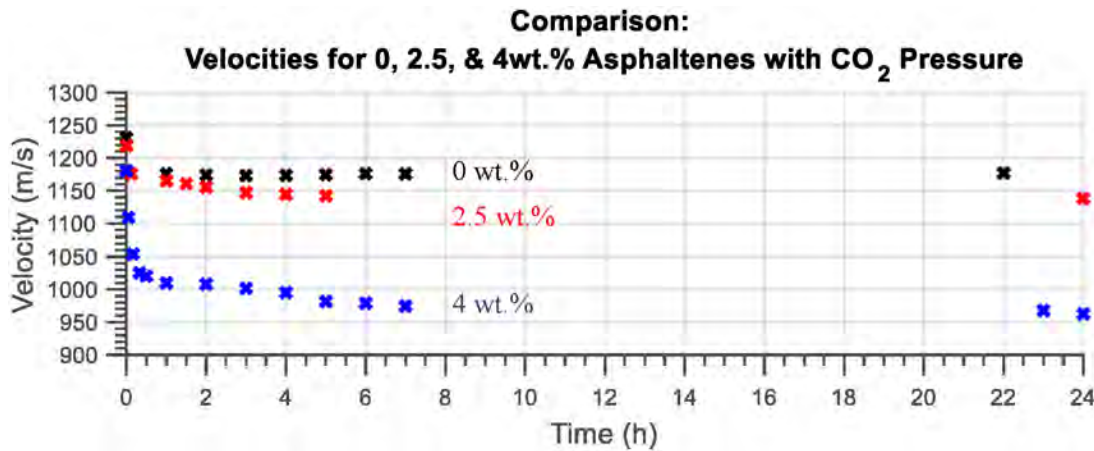


Figure 3—Ultrasonic velocities for pressurized model oils (toluene 70% - heptane 30%) with 0 (black), 2.5 (red), and 4 (blue) wt.% of N1 -C asphaltenes.

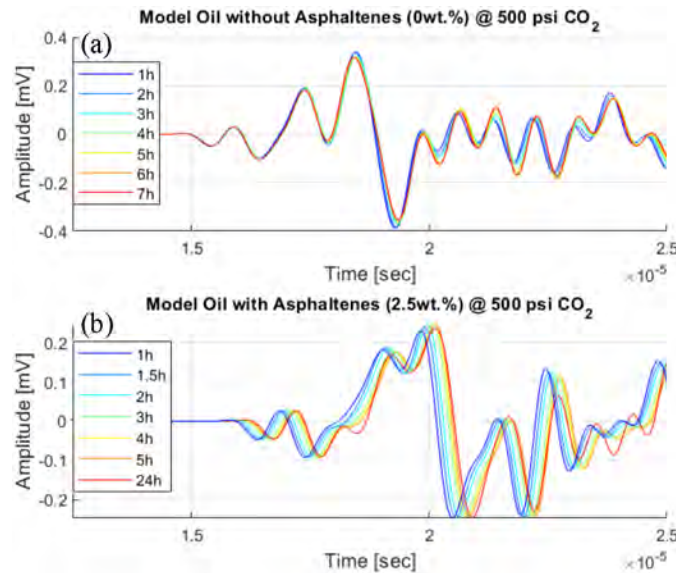


Figure 4—Continuously recorded ultrasonic waveforms for pressurized (500 psi CO₂) model oil without asphaltene and (b) model oil containing 2.5 wt.% N1-C asphaltene.

It is noted that besides asphaltene precipitation, CO₂ could induce other levels of asphaltene aggregation, namely formation of nanoaggregates and clusters, as shown by Yen-Mullins’ model in Figure 1.

At low concentration, asphaltene are generally present in crude oil as a molecular solution. Nanoaggregates (~six molecules) and clusters (~8 nanoaggregates) occur when the asphaltene concentration is increased, or the oil composition is changed to reduce asphaltene solubility.

The acoustic wave contains information of the entire fluid mixture (model oil with 70% toluene and 30% heptane + precipitated asphaltene from crude N1-C) and is therefore directly affected by the precipitated asphaltene and the presence of CO₂ (Figure 4). Moreover, although the changes are small after the 2h mark (with respect to acoustic velocities), those changes still indicate that additional asphaltene are either continuously being precipitated, or the asphaltene start to form more complex / larger structures. Both possibilities could explain the changes observed in the waveforms (Figure 4b).

Asphaltene detection through nuclear magnetic resonance (NMR)

NMR T2 relaxation curves are shown in Figure 5 for crude oil N1-A with and without asphaltene. Precipitated asphaltene cause a faster relaxation time compared to the same oil without asphaltene. Longer

relaxation times indicate that protons spin longer. In the presence of asphaltenes the protons cannot spin as freely, which results in a faster relaxation (Prunelet et al., 2004).

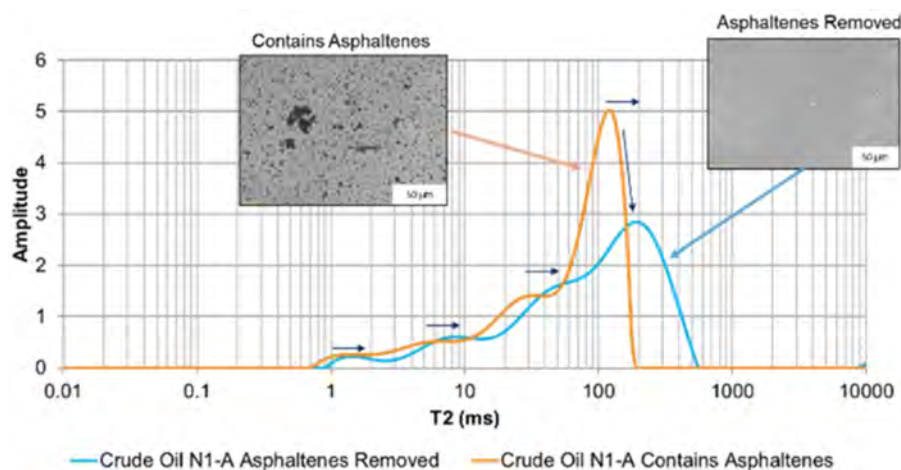


Figure 5—T₂ relaxation curves for crude oil N1-A with (orange) and without (blue) asphaltenes.

Time-lapse NMR measurements were conducted on model oil system with 30% toluene, 70% heptane and 2 wt.% asphaltene content. In this mixture ratio, the asphaltenes are unstable and precipitate, as inferred from the recorded T₂ relaxation spectra in Figure 6. The model oil system (toluene 30% - heptane 70%) without added asphaltenes shows the longest relaxation time and a single peak. Addition of asphaltenes to the model oil alters the relaxation peak. Asphaltenes in the model oil result in reduced relaxation time and amplitude. A second relaxation peak develops as asphaltenes start to precipitate (Prunelet et al., 2004). The T₂ response for the model oil with 2 wt.% asphaltenes shows a bimodal distribution pattern. After 17h the 2 peaks started to separate clearly with the larger peak at longer relaxation times approaching the model oil and the smaller peak relaxes faster by 300 ms, from about 700 ms to 400 ms in Figure 6.

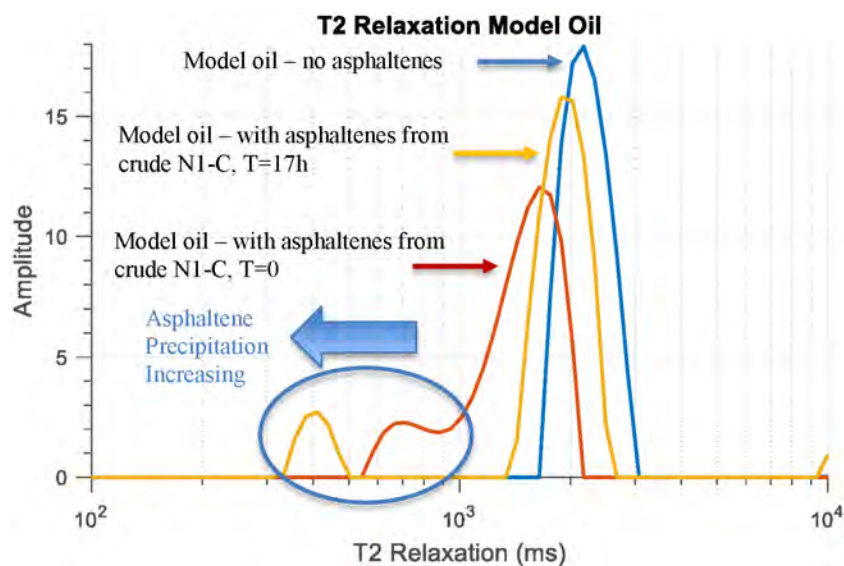


Figure 6—T₂ relaxation spectrum for model oil (toluene 30%-heptane 70%) without asphaltenes (blue curve), and model oil (toluene 30% - heptane 70%) with 2 wt.% of asphaltenes at time zero (red curve) and after 17h (yellow curve). Asphaltenes in the model oil act to reduce relaxation time and amplitude. Asphaltene precipitation is inferred from the second relaxation peak marked by a blue circle.

NMR relaxation spectrum for model oil (toluene 30% – heptane 70%) containing 2.5 wt.% of asphaltenes from crude N1-C at ambient and pressurized with 500 psig of CO₂ can be seen in Figure 7. At ambient pressure, the observed bi-modal distribution (Figure 7a) is consistent with a decrease in relaxation time due to dissolved asphaltene observed in Figure 6. After pressurizing the model oil with 500 psig of CO₂, a trimodal distribution was observed in the relaxation spectrum (Figure 7b). One can hypothesize that the peak at around 10,000 ms correlates to the bulk fluid with the residual dissolved asphaltenes and the faster relaxing peaks (~300 ms and 2,000 ms) correspond to relaxations of the model oil on the surfaces of the precipitated asphaltenes.

T₂ relaxation for model oil (toluene 70% - heptane 30%) with known amounts of N1-C asphaltenes (0, 1, 2.5, and 4 wt.%) was measured before and during exposure of 500 psig of CO₂ gas (Figure 8 and Figure 9). The model oil containing dissolved asphaltenes (Figure 8a) shows a slightly faster relaxation spectrum (1760 ms) when compared to the same model oil without asphaltenes (2230 ms) (Figure 8b). After CO₂ pressure was increased to 500 psi, two additional peaks at faster relaxation times (Figure 8c) appeared and increased in magnitude over time. The peak at longer relaxation times increases with time to longer relaxations. The blank sample [only model oil (toluene 70% - heptane 30%) without asphaltenes] shows only minimal changes in T₂ amplitudes (Figure 8d) when 500 psig of CO₂ is applied. Note that the T₂ relaxation in the model oil changes from about 2400 ms (Figure 8b) to almost 12,000 ms at 500 psi of CO₂ pressure (Figure 8d). This change is more likely due to viscosity changes and not due to a separation of the fluid phases, which should lead to a bimodal distribution.

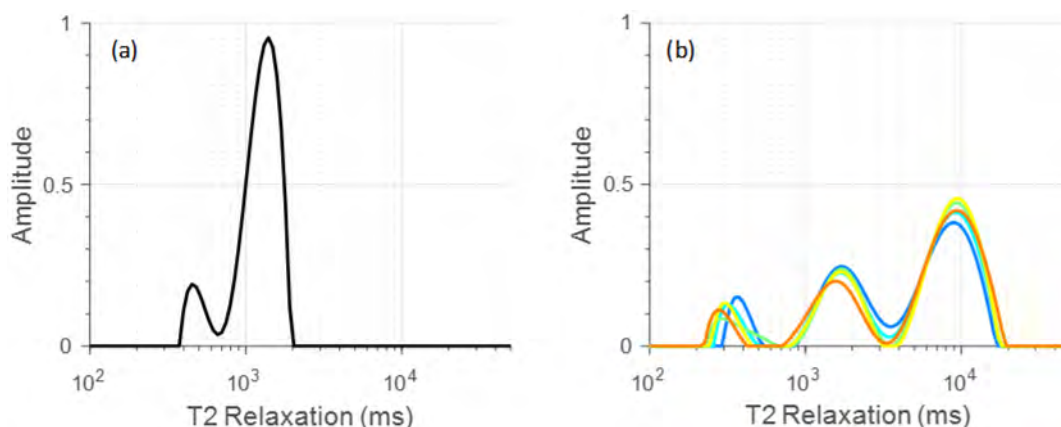


Figure 7—T₂ relaxation spectrum for model oil (toluene 30%-heptane 70%) with 2.5 wt.% crude N1-C asphaltenes at (a) ambient pressure and (b) at 500 psig of CO₂ over time. Colder colors to warmer colors indicate time progression.

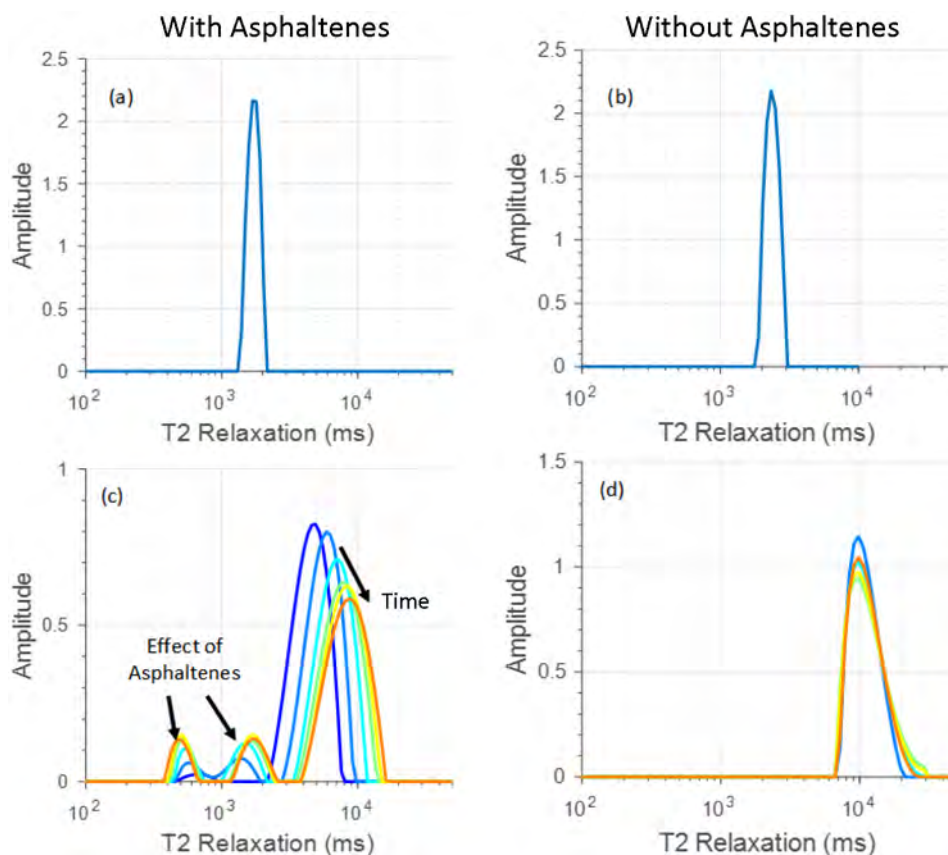


Figure 8—T2 relaxation spectra for (a) model oil (toluene 70% and heptane 30%) with 2.5 wt.% crude N1-C asphaltenes at ambient pressure (b) model oil without asphaltenes at ambient pressure (c) model oil with 2.5 wt.% crude N1-C asphaltenes from 1 to 7 h of CO₂ pressure (500 psig) and (d) model oil without asphaltenes from 2 to 6 h of CO₂ pressure (500 psig). Colder colors to warmer colors indicate time progression.

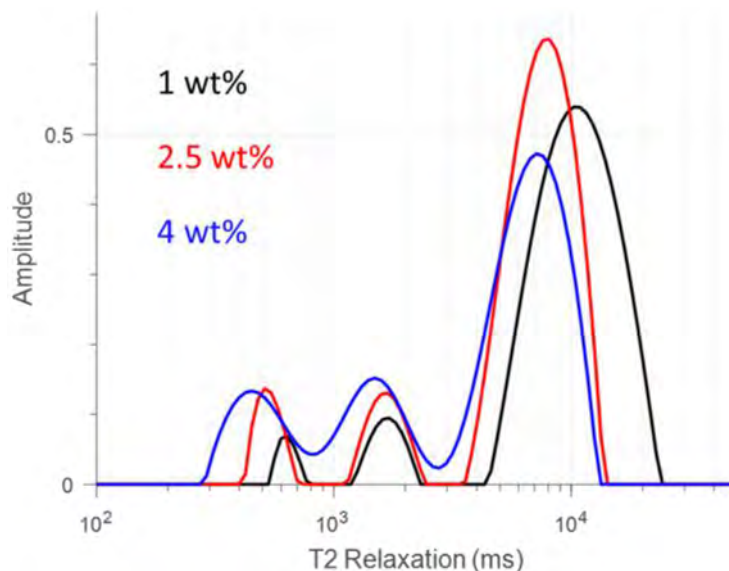


Figure 9—T2 relaxation spectra for model oil (toluene 70% – heptane 30%) and 1 wt.% (black line), 2.5 wt.% (red line), and 4 wt.% (blue line) asphaltene content. The data were collected after 4h of injection CO₂ rich gas at 500 psig.

It can be inferred that faster relaxation times around 300 ms and 1500 ms may arise from surface relaxation on the precipitated asphaltenes. This surface relaxation is expected to be at faster relaxation times (Prunelet et al., 2004) (Figure 8 and Figure 9). The CO₂ exposure induced the asphaltene precipitation from

the dissolved stage. After the CO₂ gas pressure was reduced back to ambient pressure, the two additional peaks disappeared again indicating that the precipitated asphaltenes are re-dissolved into the model oil. Figure 9 shows that the amplitudes of the T2 relaxation spectrum that correspond to the precipitated asphaltenes (signal below 3000 ms) are directly correlated to the initial asphaltene content in the model oil.

Emulsion Stability with Hydrates. HP-DSC measurements

The thermogram of the HP-DSC investigation (heating path) for the 30 vol.% water content emulsion (crude N1-C) with 10 wt.% of NaCl at 1000 psi of natural gas is shown in Figure 10. In this test, the agglomerated hydrate particle will dissociate into larger water droplets compared to the initial water droplet. As such, in the subsequent formation cycle, there will be less hydrate formation due to the lower total surface area of water droplets. Thus, the stability of the emulsion with hydrate formation/dissociation can be determined by evaluating the amount of hydrate formed in each cycle. As can be seen in Figure, the intensity of hydrate dissociation peak in the first cycle is larger compared to the intensity of the hydrate dissociation peak in the second and third cycles. This is an indication that there was significant hydrate agglomeration occurring in the system (Lachance, 2008).

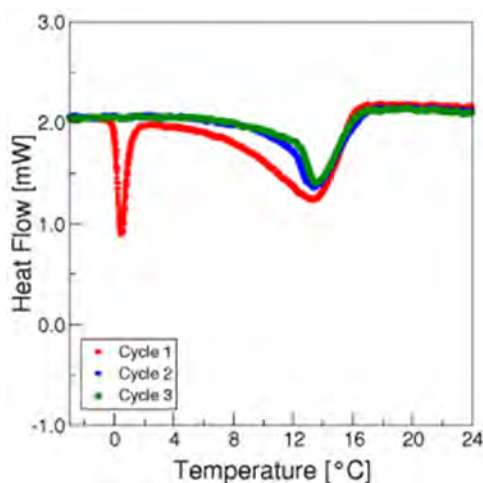


Figure 10—HP-DSC results for a water-in crude oil (N1-C) emulsion with 30% water cut and 10 wt.% NaCl. Cycle 1 (red), cycle 2 (blue), cycle 3 (green).

High pressure rheological measurements of hydrate slurry flow

The relative viscosity profile as a function of time of gas hydrate slurries formed using 30 and 50 vol.% water cut emulsions of crude N1-C, and at 1000 psig and are shown in Figure 11. These tests were conducted at 5 and 10 wt.% salinity (NaCl). The tests conducted at 10 wt.% NaCl show only a small increase in relative viscosity due to the small volume of hydrate formed; 2 vol.% of hydrate formed in the 30 vol.% water cut test and 12 vol.% of hydrate formed in the 50 vol.% hydrate tests. On the other hand, there was a higher increase in relative viscosity for the test conducted at 50 vol.% water and 5 wt.% NaCl. The higher increase in relative viscosity was due to the higher amount of hydrate formed; 23 vol.% of hydrates formed in this slurry. The lower amount of hydrates formed in the 10 wt.% NaCl tests was as expected due to lower hydrate subcooling. The subcooling for 10 wt.% NaCl tests is ~9.2 °C, while the subcooling for 5 wt.% NaCl test is ~12.8 °C.

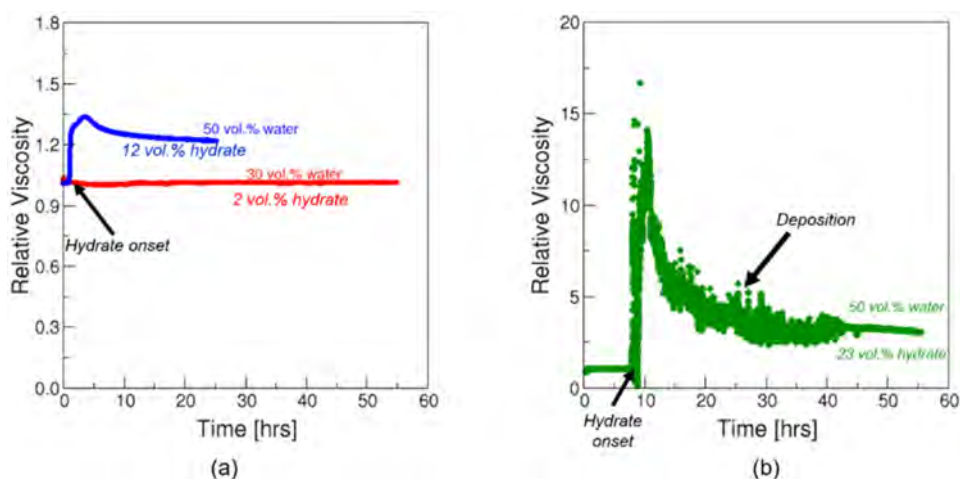


Figure 11—Viscosity profiles of hydrate slurries in crude oil N1-C formed from 30 and 50 vol. % water content emulsions at 200 RPM using the natural gas, a) 10 wt.% NaCl and, b) 5 wt.% NaCl.

Additionally, the results show larger fluctuations in the viscosity profile for tests conducted at 5 wt. % NaCl and 50 vol.% water content. From previous investigations, these fluctuations are the results of formation of severe hydrate deposits on the walls of the rheometer (Majid et al., 2019). In comparison, there were no fluctuations in the tests conducted at 10 wt.% NaCl. The absence of fluctuations indicates that there was a homogeneous distribution of hydrate particles in the slurries (Majid et al., 2019).

Next, measurements of yield stress of these hydrate slurries were also conducted (Figure 12). These tests mimic the transient conditions of shut-in and restart, which is considered at the highest risk situation for field operations. It should be noted that the yield stress was measured after the hydrate slurries were left in shut-in conditions (no stirring) for 24 hours. A summary of the yield stress values obtained from these measurements are presented in Table 4. The results indicate that higher amounts of hydrates will lead to higher yield stress values. This agrees with previous studies (Rensing, 2010; Webb et al., 2012). At higher particle concentration, the hydrate particles are more tightly packed. Thus, during the 24-hour shut-in time, the hydrate particles would sinter, and this would lead to higher yield stress values.

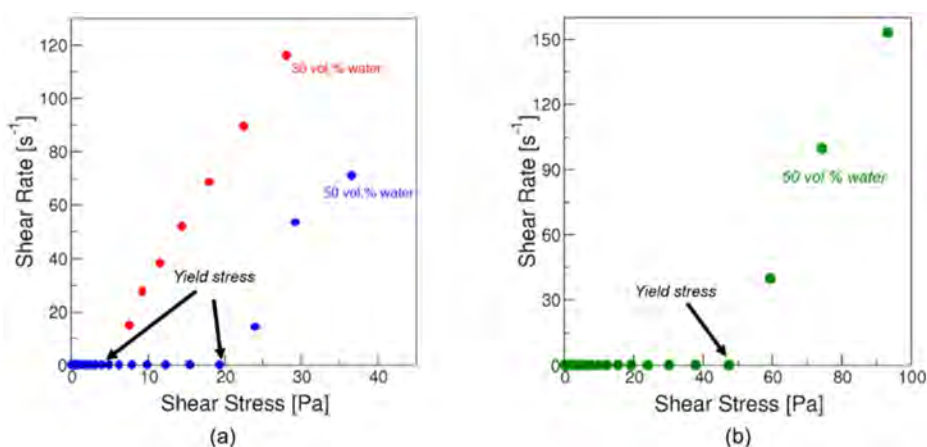


Figure 12—Yield stress of hydrate slurries in crude oil N1-C formed from 30 and 50 vol.% water content emulsions at 200 RPM for tests formed using natural gas and (a) 10 wt.%, and (b) 5 wt.% NaCl.

Table 4—Yield stress (after shut-in/restart) of hydrate slurries in crude oil N1-C formed at 1000 psig of natural gas at different water content and salinity

Water content (vol.%)	NaCl (wt.%)	Hydrate volume %	Yield stress (Pa)
30	10	2	6

Water content (vol.%)	NaCl (wt.%)	Hydrate volume %	Yield stress (Pa)
50	10	12	19
50	5	23	48

Measurements of hydrate slurry viscosity were also conducted using 50 vol.% water, 5 wt.% NaCl and the CO₂-rich natural gas. Figure 13a shows the viscosity profile of the hydrate slurries as a function of time (pink). The viscosity profile of a similar test (50 vol.% water, 5 wt.% salinity) formed from the natural gas composition (orange) is shown in the same plot for comparison. As can be seen in this plot, the viscosity of hydrate slurries formed from the CO₂-rich natural gas composition was significantly lower compared to the viscosity of hydrate slurries formed from the low-CO₂ content gas (natural gas). The lower viscosity in CO₂-rich gas composition tests was due to a phase inversion that had occurred. This phase inversion was indicated by the sharp and sudden decrease in the viscosity profile (at ~1.0 hr). It should be noted that in both tests, the system began with crude oil as the continuous phase. However, in the test using the CO₂-rich gas, the formation of hydrate caused a phase inversion, whereby the system changed from being oil continuous to water continuous. This phase inversion was confirmed by performing a dispersion test at the end of the rheometer experiment. It is hypothesized that the high CO₂ content in the gas phase lowers the pH of the water. This lower water pH activated the natural hydrophilic surfactants in the oil, which then caused the phase inversion (Poteau et al., 2005; Rodriguez-Abreu et al., 2006).

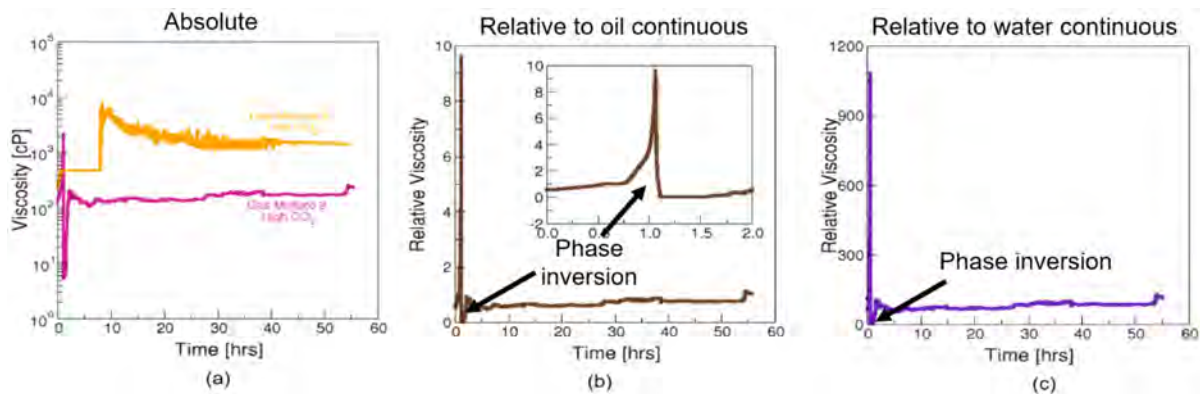


Figure 13—Viscosity profiles of hydrate slurries in crude oil N1-C formed from 50 vol.% water content, 5 wt.% salinity (NaCl) and CO₂-rich natural gas composition. (a) Absolute viscosity, (b) relative viscosity (relative to oil phase) and (c) relative viscosity (relative to water phase).

Figures 13b and c show two different analyses of the viscosity profiles. In Figure 13b, relative viscosity was determined with respect to oil as the continuous phase; while in Figure 13c, viscosity was determined relative to water as the continuous phase. The relative viscosity with respect to water as the continuous phase showed a significantly higher value. In this test, relative viscosity should be determined with respect to the water phase due to phase inversion that had occurred. This would provide a better representation of the effect of hydrate particles on the viscosity of the slurries.

Conclusions

Early detection of asphaltene precipitation and deposition and hydrate formation at field conditions is critical for industry to minimize/optimize the application of mitigation/remediation strategies. In this work, the asphaltene precipitation was determined using acoustic measurements and nuclear magnetic resonance (NMR). Asphaltene particles changed the velocity of the acoustic wave travelling through the sample. Similar results were found for crude oil and model (toluene-heptane) systems. The magnitude of the acoustic

velocity change seems to be dependent on the initial asphaltene concentration in the systems, which is a promising finding considering the possibility of a further quantification of the amount of precipitated asphaltenes. NMR T2 relaxation time curves were different for systems with precipitated asphaltenes as compared to systems without precipitation. Precipitated asphaltenes could be associated with a characteristic peak observed on NMR T2 profiles, however the location of that peak depends on the conditions of the system. NMR was sensitive to the initial concentration of asphaltenes. It is worth noting that both experimental techniques, acoustic measurements, and NMR, were able to detect asphaltene precipitation with high pressure of CO₂, which shows their potential application in the field.

The assessment of the rheological properties of gas hydrate slurries was carried out in a high-pressure rheometer. The system composed of natural gas and crude oil N1-C exhibited hydrate agglomeration at high water content (50 vol.%) and 5 wt.% NaCl, which was due mainly to the large amount of hydrates formed. Likewise, the yield stress of this system was also higher than those corresponding to the systems with 10 wt.% NaCl. The plugging behavior of this crude oil could be associated with the low emulsion stability observed when hydrates are present. The viscosity of the hydrate slurry formed in the system with 50 vol. % water and a CO₂-rich gas was significantly lower than the viscosity of the system using a natural gas (with low-CO₂ content) and the same water vol.%, which was due to a phase inversion phenomenon. This inversion has not been reported previously and may be explained by the reduction in the water pH induced by the CO₂ dissolution.

Acknowledgements

The authors acknowledge Nippon Foundation - DeepStar® Partnership for providing funding and support for this work through the project DeepStar® 20122. Champions of this project, Douglas Estanga (Chevron), Giovanni Grasso (ExxonMobil), Joe Lederhos (ExxonMobil), Daniel Crosby (Shell), Adriana Teixeira (Petrobras), Leandro Valim (Petrobras), Nakano Yoshitaka (JX) and Ushiguchi Kento (JX) are acknowledged for their technical support and advise.

References

- Aguilera, B., Delgado, J., & Cárdenas, A. 2010. Water-in-Oil emulsions stabilized by asphaltenes obtained from Venezuelan crude oils. *Journal of Dispersion Science and Technology*, **31**(3), 359–363.
- Alimohammadi, S., Zendejboudi, S., & James, L. 2019. A Comprehensive Review of Asphaltene Deposition in Petroleum Reservoirs: Theory, challenges, and tips. *Fuel*, **252**, 753–791. <https://doi.org/10.1016/j.fuel.2019.03.016>
- Buckley, J. S., Wang, J., & Creek, J. L. 2007. Solubility of the Least-Soluble Asphaltenes. In O. C. Mullins, E. Y. Sheu, A. Hammami, & A. G. Marshall (Eds.), *Asphaltenes, Heavy Oils, and Petroleomics* (pp. 401–437). Springer New York. https://doi.org/10.1007/0-387-68903-6_16
- Chen, L., Bertolini, A., Dubost, F., Achourov, V., Betancourt, S., Cañas, J. A., Dumont, H., Pomerantz, A. E., & Mullins, O. C. 2020. Yen-Mullins Model Applies to Oilfield Reservoirs. *Energy & Fuels*, **34**(11), 14074–14093. <https://doi.org/10.1021/acs.energyfuels.0c02937>
- Czarnecki, J., & Moran, K. 2005. On the Stabilization Mechanism of Water-in-Oil Emulsions in Petroleum Systems. *Energy & Fuels*, **19**(5), 2074–2079. <https://doi.org/10.1021/ef0501400>
- da Silva, N. A. E., da Oliveira, V. R. R., Souza, M. M. S., Guerrieri, Y., & Costa, G. M. N. 2014. New method to detect asphaltene precipitation onset induced by CO₂ injection. *Special Issue on PPEPPD 2013*, **362**, 355–364. <https://doi.org/10.1016/Zj.fluid.2013.10.053>
- Delgado-Linares, J. G., Costa Salmin, D., Stoner, H., Wu, D. T., E. Zerpa, Koh, C.L.A., Mateen, K., Bodnar, S., Prince, P., & Teixeira, A. 2020. Effect of Alcohols on Asphaltene-Particle Size and Hydrate Non-Plugging Behavior of Crude Oils. *OTC-30916-MS*, 13. <https://doi.org/10.4043/30916-MS>
- Delgado-Linares, J. G., Majid, A. A. A., Zerpa, L. E., & Koh, C. A. 2021. Reducing THI Injection and Gas Hydrate Agglomeration by Under-Inhibition of Crude Oil Systems. D031S038R007. <https://doi.org/10.4043/31161-MS>
- Delgado-Linares, J. G., Majid, A. A., Sloan, E. D., Koh, C. A., & Sum, A. K. 2013. Model waterin-oil emulsions for gas hydrate studies in oil continuous systems. *Energy & Fuels*, **27**(8), 4564–4573.
- Deo, M., & Parra, M. 2012. Characterization of Carbon-Dioxide-Induced Asphaltene Precipitation. *Energy & Fuels*, **26**(5), 2672–2679. <https://doi.org/10.1021/ef201402v>

- Ellison, B. T., Gallagher, C. T., Frostman, L. M., & Lorimer, S. E. 2000. The Physical Chemistry of Wax, Hydrates, and Asphaltene. <https://doi.org/10.4043/11963-MS>
- Fakher, S., Ahdaya, M., Elturki, M., & Imqam, A. 2020. An Experimental Investigation of Asphaltene Stability in Heavy Crude Oil During Carbon Dioxide Injection. *Journal of Petroleum Exploration and Production Technology*, **10**(3), 919–931. <https://doi.org/10.1007/s13202-019-00782-7>
- Gharbi, K., Benyounes, K., & Khodja, M. 2017. Removal and prevention of asphaltene deposition during oil production: A literature review. *Journal of Petroleum Science and Engineering*, **158**, 351–360.
- Gudmundsson, J. S. 2017. Flow Assurance Solids in Oil and Gas Production. CRC Press/Balkema.
- Hammami, A., & Ratulowski, J. 2007. Precipitation and Deposition of Asphaltenes in Production Systems: A Flow Assurance Overview. In O. C. Mullins, E. Y. Sheu, A. Hammami, & A. G. Marshall (Eds.), *Asphaltenes, Heavy Oils, and Petroeomics* (pp. 617–660). Springer New York. https://doi.org/10.1007/0-387-68903-6_23
- Jamaluddin, A. K. M., Creek, J., Kabir, C. S., McFadden, J. D., D'Cruz, D., Manakalathil, J., Joshi, N., & Ross, B. 2002. Laboratory Techniques to Measure Thermodynamic Asphaltene Instability. *Journal of Canadian Petroleum Technology*, **41**(07) <https://doi.org/10.2118/02-07-04>
- Kelland, M. A. 2016. Production Chemicals for the Oil and Gas Industry. CRC Press.
- Kinnari, K., Hundseid, J., Li, X., & Askvik, K. M. 2014. Hydrate Management in Practice. *Journal of Chemical & Engineering Data*, **60**(2), 437–446.
- Kokal, S. L. 2005. Crude Oil Emulsions: A State-Of-The-Art Review. *Society of Petroleum Engineers*. <https://doi.org/10.2118/77497-PA>
- Lachance, J. 2008. Investigation of Gas Hydrates Using Differential Scanning Calorimetry with Water-in-Oil Emulsions. Master Thesis. Colorado School of Mines.
- Lei, H., Pingping, S., Ying, J., Jigen, Y., Shi, L., & Aifang, B. 2010. Prediction of asphaltene precipitation during CO₂ injection. *Petroleum Exploration and Development*, **37**(3), 349–353. [https://doi.org/10.1016/S1876-3804\(10\)60038-9](https://doi.org/10.1016/S1876-3804(10)60038-9)
- Livo, K., Prasad, M., & Graham, T. R. 2021. Quantification of Dissolved O₂ in Bulk Aqueous Solutions and Porous Media Using NMR Relaxometry. *Scientific Reports*, **11**(1), 290. <https://doi.org/10.1038/s41598-020-79441-5>
- Majid, A. A. A., Creek, J., Subramanian, S., Estanga, D. A., & Koh, C. A. 2021. Rapid Screening Method for Hydrate Agglomeration and Plugging Assessment Using High Pressure Differential Scanning Calorimetry. *Fuel*, **306**, 121625. <https://doi.org/10.1016/j.fuel.2021.121625>
- Majid, A. A., Tanner, B., & Koh, C. A. 2019. Cyclopentane Hydrate Slurry Viscosity Measurements Coupled with Visualisation. *Molecular Physics*, 1–11.
- Majid, A. A., Wu, D. T., & Koh, C. A. 2017. New in situ measurements of the viscosity of gas clathrate hydrate slurries formed from model water-in-oil emulsions. *Langmuir*, **33**(42), 11436–11445.
- McLean, J. D., & Kilpatrick, P. K. 1997. Effects of Asphaltene Solvency on Stability of WaterIn-Crude-Oil Emulsions. *Journal of Colloid and Interface Science*, **189**(2), 242–253.
- Mullins, O. C. 2011. The Asphaltenes. *Annual Review of Analytical Chemistry*, **4**, 393–418.
- Poteau, S., Argillier, J.-F., Langevin, D., Pincet, F., & Perez, E. 2005. Influence of pH on Stability and Dynamic Properties of Asphaltenes and Other Amphiphilic Molecules at the Oil-Water Interface. *Energy & Fuels*, **19**(4), 1337–1341. <https://doi.org/10.1021/ef0497560>
- Prunelet, A., Fleury, M., & Cohen-Addad, J.-P. 2004. Detection of asphaltene Flocculation Using NMR Relaxometry. *Comptes Rendus Chimie*, **7**(3-4), 283–289.
- Rensing, P. 2010. Studies of the Rheology of Ice and Clathrate Hydrate Slurries Formed in Situ from Water-In-Oil Emulsions. PhD Thesis. Colorado School of Mines.
- Rensing, P. J., Liberatore, M. W., Sum, A. K., Koh, C. A., & Sloan, E. D. 2011. Viscosity And Yield Stresses of Ice Slurries Formed in Water-In-Oil Emulsions. *Journal of NonNewtonian Fluid Mechanics*, **166**(14-15), 859–866.
- Reyes Molina, E. A., Delgado-Linares, J. G., Cárdenas, A. L., & Forgiarini, A. M. 2021. Foamability of non-aqueous systems containing asphaltenes from a heavy crude oil. *Petroleum Science and Technology*, **39**(11-12), 430–440. <https://doi.org/10.1080/10916466.2021.1919706>
- Rodriguez-Abreu, C., Delgado-Linares, J. G., & Bullon, J. 2006. Properties of Venezuelan Asphaltenes in the Bulk and Dispersed State. *Journal of Oleo Science*, **55**(11), 563–571. <https://doi.org/10.5650/jos.55.563>
- Salmin, D. C., Delgado-Linares, J. G., Wu, D. T., Zerpa, L. E., & Koh, C. A. 2021. Hydrate Agglomeration in Crude Oil Systems in Which the Asphaltene Aggregation State Is Artificially Modified. *SPE Journal*, **26**(03), 1189–1199. <https://doi.org/10.2118/204456-PA>
- Sjöblom, J., Øvrevoll, B., Jentoft, G., Lesaint, C., Palermo, T., Siquin, A., Gateau, P., Barré, L., Subramanian, S., Boxall, J., Simon, D., Dieker, L., Greaves, D., Lachance, J., Rensing, P., Miller, K., Sloan, E. D., & Koh, C. A. 2010. Investigation of the hydrate plugging and nonplugging properties of oils. *Journal of Dispersion Science and Technology*, **31**(8), 1100–1119.
- Sloan, E. D. 2010. Natural gas hydrates in flow assurance. Gulf Professional Publishing.

- Sloan, E. D., & Koh, C. A. 2007. Clathrate hydrates of natural gases. CRC press.
- Speight, J. 2004. Petroleum Asphaltenes-Part 1: Asphaltenes, Resins and The Structure of Petroleum. *Oil & Gas Science and Technology*, **59**(5), 467–477.
- Spiecker, P. M., Gawrys, K. L., & Kilpatrick, P. K. 2003. Aggregation and Solubility Behavior of Asphaltenes and Their Subfractions. *Journal of Colloid and Interface Science*, **267**(1), 178–193. [https://doi.org/10.1016/S0021-9797\(03\)00641-6](https://doi.org/10.1016/S0021-9797(03)00641-6)
- Sum, A. K., Koh, C. A., & Sloan, E. D. 2012. Developing a Comprehensive Understanding and Model of Hydrate in Multiphase Flow: From Laboratory Measurements to Field Applications. *Energy & Fuels*, **26**(7), 4046–4052. <https://doi.org/10.1021/ef300191e>
- Wang, Z., Xu, J., Liu, H., Hou, J., & Zhang, Y. 2017. Effect of Pressure, Temperature, and Mass Fraction of CO₂ on the Stability of the Asphaltene Constituents in Crude Oil. *Petroleum Science and Technology*, **35**(22), 2109–2114. <https://doi.org/10.1080/10916466.2017.1384838>
- Webb, E. B., Rensing, P. J., Koh, C. A., Sloan, E. D., Sum, A. K., & Liberatore, M. W. 2012. High-Pressure Rheology of Hydrate Slurries Formed From Water-In-Oil Emulsions. *Energy & Fuels*, **26**(6), 3504–3509.
- Zanganeh, P., Ayatollahi, S., Alamdari, A., Zolghadr, A., Dashti, H., & Kord, S. 2012. Asphaltene Deposition during CO₂ Injection and Pressure Depletion: A Visual Study. *Energy & Fuels*, **26**(2), 1412–1419. <https://doi.org/10.1021/ef2012744>